Reaction of $O_2^+ + C_8H_{10}$ (Ethylbenzene) as a Function of Pressure and Temperature: A Study of the Collisional Stabilization of the Reactant Intermediate

A. A. Viggiano,*,† Thomas M. Miller,† Skip Williams,† Susan T. Arnold,† John V. Seeley,‡ and Jeffrey F. Friedman§,||

Air Force Research Laboratory, Space Vehicles Directorate, 29 Randolph Road, Hanscom AFB, Massachusetts 01731-3010, Department of Chemistry, Oakland University, Rochester, Michigan 48309, and Air Force Research Laboratory, Directed Energy Directorate, Kirtland AFB, New Mexico 87117-5776

Received: August 16, 2002; In Final Form: September 27, 2002

Rate constants and branching fractions for the reaction of O_2^+ with C_8H_{10} (ethylbenzene) have been measured in the recently upgraded turbulent ion flow tube (TIFT) and are reported here as a function of temperature from 423 to 573 K and number density from 3×10^{17} to 25×10^{17} molecules cm^{-3}. The results reported here represent the first measurements to be made on this instrument as a function of both temperature and pressure. The rate constants for the reaction of O_2^+ with C_8H_{10} are collisional and exhibit no appreciable variation with temperature or pressure. The reaction proceeds primarily by dissociative and nondissociative charge transfer forming two main product ions, namely, $C_8H_{10}^+$ and $C_7H_7^+$. The ratio of $[C_8H_{10}^+]$ to $[C_7H_7^+]$ depends strongly on both the buffer gas number density and the temperature. Increasing the number density increases the abundance of $C_8H_{10}^+$, indicating that collisional stabilization of the charge transfer excited state is occurring. Measurements were made using both He and N_2 buffers. Nitrogen is almost twice as efficient at stabilizing the charge transfer product than is He. A simple model predicts the ratio of $[C_8H_{10}^+]$ to $[C_7H_7^+]$ to depend linearly on number density, which is consistent with the experimental results. At a constant number density, the abundance of $C_7H_7^+$ increases with temperature. A small amount of thermal dissociation of $C_8H_{10}^+$ has been observed at 573 K.

Introduction

Recent results from our laboratory on the reactions of ions with aromatic molecules indicate that the buffer gas plays an important role in many reactions. A comparison of the product breakdown curves obtained from low-pressure photodissociation experiments with those obtained from charge transfer reactions at about 0.5 Torr showed that the higher pressure threshold energy for dissociation was shifted over an electronvolt to higher energy for both benzene and naphthalene cations.[1−4] Part of the shift was attributed to the helium buffer stabilizing the excited charge transfer products, $(C_6H_6^+)^*$ and $(C_{10}H_8^+)^*$, before they could dissociate. Both cations are known to have long lifetimes near the threshold for dissociation.[5,6] Similar but smaller effects were observed in reactions with alkylbenzenes.[7] The buffer was thought to play a different role in reactions between $H_3O^+(H_2O)$ and alkylbenzenes,[8] adding energy for dissociation to occur. This may occur in interactions with either the reactant intermediate or the proton transfer product. The latter process is thermal dissociation and has been observed in other reactions as well.[9−15] Thus, the buffer gas can stabilize or destabilize parent ions.

The studies from our laboratory described above were made using both a high-temperature flowing afterglow and a selected ion flow tube. Because the buffer gas pressure could not be varied dramatically, the effects attributed to the buffer were mostly speculative. Recently, we have constructed a turbulent ion flow tube (TIFT) for studying ion reactivity at elevated pressures, 10−700 Torr. In the first two studies, only room temperature kinetics were reported.[16,17] Instrument modifications have been completed that now allow for temperature studies from 300 to 573 K, and future improvements should increase the temperature range by 200−300 K. Thus, a more thorough evaluation is now possible for some of the previously proposed reaction mechanisms involving the buffer gas.

The above discussion illustrates that pressure effects should be important in numerous systems. However, for an initial study, the chemistry should be as simple as possible and several criteria were considered. The reactant ion had to be easily produced at high pressure without significant impurities. Although O_2^+ and NO^+ both fit this category, NO^+ generally reacts only by nondissociative charge transfer; therefore, reactions involving NO^+ were not expected to have large pressure dependences except at temperatures where the charge transfer product might thermally decompose. Once the TIFT can reach higher temperatures, NO^+ may be a good reactant ion for studies involving decomposition by the buffer gas. In previous studies, rate constants were often collisional and would not be expected to be temperature- or pressure-dependent. Therefore, a good candidate for study would be a reaction of O_2^+ for which both nondissociative and dissociative charge transfer processes occurred. Ideally, only one dissociative process would be important. The reaction of O_2^+ with ethylbenzene (C_8H_{10}) fits

* To whom correspondence should be addressed.
† Air Force Research Laboratory, Space Vehicles Directorate.
‡ Oakland University.
§ Air Force Research Laboratory, Directed Energy Directorate.
|| Permanent address: Department of Physics, University of Puerto Rico-Mayaguez, Mayaguez, PR 00681-9016.

10.1021/jp026780a CCC: $22.00
Published on Web 11/12/2002

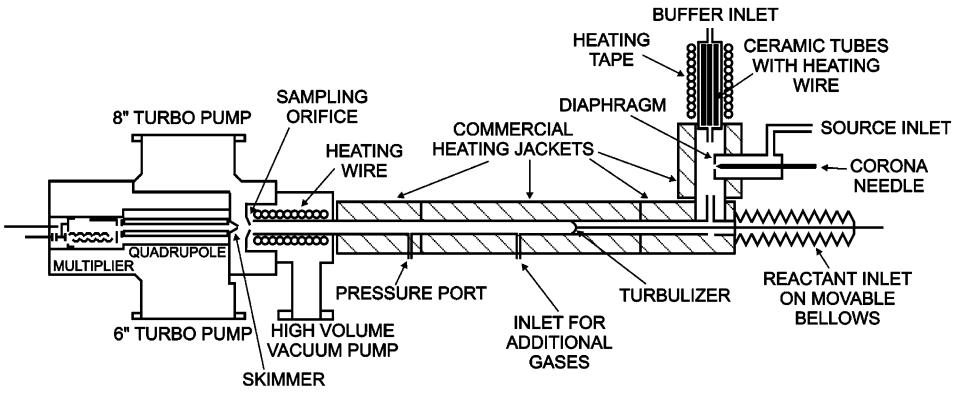

Figure 1. Schematic of the TIFT as modified for extended temperature studies.

these criteria. By far, the two most important product channels (>95%) are[7,18]

$$O_2^+ + C_8H_{10} \rightarrow C_8H_{10}^+ + O_2 + 3.31\ \text{eV} \quad (1)$$

$$\rightarrow C_7H_7^+ + CH_3 + O_2 + 2.08\ \text{eV}$$

The thermochemistry of reaction 1 is such that the dissociation channel is significantly above threshold. Although $C_6H_6^+$ and $C_8H_9^+$ are formed in very small amounts at low pressure, they can be ignored for this initial study since their abundance is on the order of impurity ions. Therefore, the most interesting parameter to study as a function of pressure is the ratio (R) of $C_8H_{10}^+$ to $C_7H_7^+$ product abundances. If the lifetime of the excited charge transfer product, $(C_8H_{10}^+)^*$, is long as compared to the collisional lifetime with respect to the buffer gas, then the branching should depend on pressure. On the basis of lifetimes for the similar species, $C_7H_8^+$ and $C_9H_{12}^+$,[19,20] it may be expected that the lifetime would be comparable to the collision time with the bath gas, although the energy content of the charge transfer product is not known. In this paper, measurements of R as a function of pressure at temperatures from 423 to 573 K in a N_2 buffer are reported as well as a few measurements made using a He buffer. Rate constants were also measured under many of the conditions, but no variation was found. The temperature and pressure limits were determined by the allowable intensity of impurity ions (at low temperature and high pressure), experimental problems in heating (at high temperature), and ion signal (at low pressure).

Experimental Section

Operation of the TIFT at room temperature has been described previously.[16] Details of the upgrades necessary for extended temperature operation are given here. The instrument was operated similarly to low-pressure flow tubes except that the gas flow was much larger so that the Reynolds number (R_N) was much higher. In fact, the same software ran the TIFT, the selected ion flow tube, and high-temperature flowing afterglow in our laboratory. When possible, the TIFT was run in or near the turbulent flow regime, which occured for $R_N > 3000$. The primary reason to operate at higher R_N was that the introduction of the reactant neutral into the buffer gas benefited from the turbulent mixing. This was not critical for measuring branching ratios since only relative ion signals taken under similar conditions were important. Therefore, not all of the present experiments were performed in the turbulent flow regime in order to save on buffer gas. In addition, at lower pressures, it was not possible to operate in the turbulent regime due to pumping speed limitations.

The modified TIFT for high-temperature operation is shown in Figure 1. Briefly, a buffer gas, usually N_2 from liquid N_2, was introduced into a stainless steel flow tube (i.d. = 1 in). For the limited data obtained in a He buffer, the He was passed through three liquid nitrogen traps filled with molecular sieves to remove H_2O. It was necessary to reheat the He before the flow reached the flow controller. Ions were created upstream in an off-axis corona discharge source and mixed into the upstream end of the flow tube. A one-fourth inch on-axis movable tube introduced the neutral reagent. The inlet can be moved 60 cm within the flow tube. The bulk of the gas was pumped away by a large mechanical pump, and a small amount of gas was sampled through an orifice, variable between 50 and 200 μm, in a truncated cone. A supersonic expansion occured behind the orifice, and the core of the expansion was sampled into a mass spectrometer by a conical skimmer. Voltages were applied to the sampling cone and skimmer. The ions were mass-selected with a quadrupole mass filter and counted by a discrete dynode electron multiplier.

Retrofitting the instrument for high-temperature operation required six zones of heating. All zones were maintained to $\pm 2-4$ K by Watlow heating controllers. The main flow tube was heated in four zones, two short zones at the ends of the flow tube, a long center section, and a zone inside the vacuum chamber that heated the very end of the flow tube. Except for the zone inside the vacuum, the heaters were commercial components from Amptek, which had built-in thermocouples and insulation. The inside zone was made from Nichrome wire surrounded by ceramic tubes. The buffer gas and ions were introduced through a sidearm in the upstream end of the flow tube. The tube connected to the sidearm housing a corona ion source was also heated by an Amptek heater.

The buffer gas must be preheated since there was not enough residence time in the flow tube for the buffer to reach thermal equilibrium with the walls before the reaction zone.[21] Heating the buffer was accomplished by inserting Nichrome wire into ceramic rods, which were then packed into a stainless steel tube. The tube was also heated on the outside by heating tape controlled by a Variac. We found that in order for the buffer gas to reach the proper temperature in the flow tube, the temperature of the gas exiting the buffer heater had to be hotter than the desired flow tube temperature. Therefore, a thermocouple in a 1/16 in sealed stainless steel tube was inserted into the reactant inlet to measure the buffer gas temperature. The buffer heating was then controlled to this temperature. The gas exiting the buffer heater was on the order of 30−80 K hotter than the flow tube. Temperature uniformity in the flow tube appeared to be well-maintained as moving the reactant inlet 60 cm produced at most a 2 K temperature change. The test was

performed faster than the inlet heater could respond and therefore represented the actual temperature variation. The internal heater tended to burn out, therefore we also operated with only the added heating tape to the outside of the tube. All materials were compatible with operation up to 900 K. However, a better and more reliable buffer heating method was needed to run above 573 K.

Since our earlier work on this instrument, a bellows was added upstream of the flow tube, so the reactant neutral inlet could be moved without breaking vacuum. This was an important modification since the system was very sensitive to impurities, which dissipated only slowly. For instance, any time the system was opened to atmosphere, an H_2O impurity persisted for hours to days. However, after baking at or above the operating temperature, it was possible to generate O_2^+ with greater than 99% purity at $\leq$50 Torr and with somewhat less purity at higher pressure. All of the data reported here have ion impurity levels of 3% or less. The main impurities remaining are H_3O^+, N_3^+, $O_2^+(H_2O)$, and N_4^+. At higher temperatures (>600 K at the exhaust of the buffer heater), Na^+ and K^+ were also observed.

The neutral reactant was added through a one-fourth inch tube that was attached to the endplate of the bellows. The reaction distance was varied by compressing or expanding the bellows. The tube was centered by two fan-shaped "turbulizers" at the end of the tube. These were similar to the ones described previously, except that the Teflon component was replaced by one made from stainless steel. This allowed for an extended temperature range. The turbulizers were used to mix the neutral reagent in a short distance. The end correction for mixing with this design was found to be negligible (<1−2 cm). A thermocouple probe was positioned such that the junction was just at the end of the inlet. For the experiments reported here, C_8H_{10} was introduced as a 1% mixture in N_2.

Previously, a ^{210}Po radioactive ion source was used in the TIFT. With this source, much or most of the buffer gas was passed through the source in order to obtain an appreciable ion signal. Because the materials in that source were incompatible with preheating the buffer, the ion source was replaced by a corona discharge. The design was similar to the one used in the field chemical ionization mass spectrometer developed at AFRL.[22,23] A stainless steel corona needle was inserted into an aluminum cup with a 0.125 cm diameter aperture. A 1 cm diameter circle around the aperture was anodized, which greatly improved the ion signal although the reason for this effect remains unknown. A negative potential of 1000−3000 V was applied to the needle leading to an emission current of several microamperes. Enclosing the corona in a cup ensured that the discharge occurred at high pressure, where it operated most efficiently. An O_2 flow of 0.5−3 standard liters min^{-1} was used for optimum signal levels. Higher O_2 flow rate led to more H_2O impurity, so most of the data reported here was taken with the smaller value.

Examples of mass spectra are shown in Figure 2, with and without the C_8H_{10} reactant gas. In this spectrum, O_2^+ was by far the dominant ion. The impurity ions H_3O^+ and N_3^+ were about 0.5% of the O_2^+ signal, making corrections to the branching ratios insignificant. At higher pressures, small corrections were required. With the addition of ethylbenzene, ions at mass 78, 91, 106, and 119 amu were observed. The 78 amu signal was on the order of the impurity levels and was ignored for these experiments. The 119 amu signal, which extrapolated to zero in the absence of C_8H_{10} flow, was due to the reaction of $C_7H_7^+$ with C_8H_{10}.[24] The large peak at 106 amu also

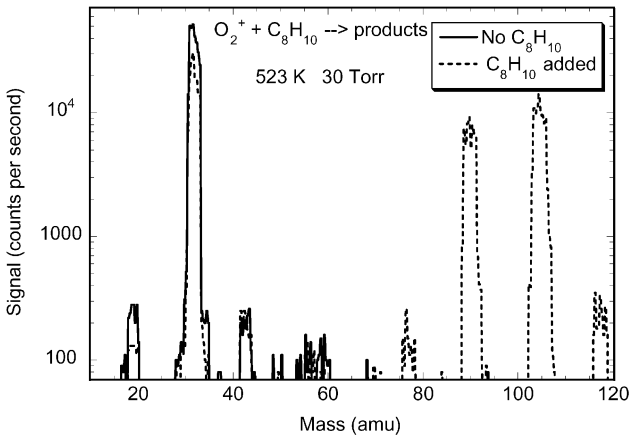

Figure 2. Mass spectra with and without added C_8H_{10} at 523 K and 30 Torr.

contained a small amount of mass 105 and mass 107. The 105 peak was on the order of the impurity level and was ignored. The 107 peak was due partly to the ^{13}C isotope of the 106 amu products and partly to a minor proton transfer product originating from the H_3O^+ impurity. Corrections were made when conditions required.

Branching ratios and rate constants were obtained by varying the flow of the neutral gas. Rate constants were derived from the decay rate with the aid of separate time-of-flight measurements as functions of both temperature and Reynolds number to determine the reaction time. Branching ratios or fractions were derived by extrapolating the fraction of each product to zero reactant flow. Extrapolating the branching fraction to zero extent of reaction eliminated any contribution due to secondary chemistry.

Numerous checks on the data were performed, primarily at 473 K. The sampling voltages were all varied, i.e., the sampling cone, skimmer, and quadrupole bias voltages. No appreciable change in the data occurred except at low skimmer voltages, where a focusing effect was found. The reaction distance was varied with no change in the rate or branching ratio, except a very small change at 573 K that appeared to be due to thermal dissociation as described below. To test for breakup in sampling, the reaction of NO^+ with C_8H_{10} was studied. This reaction had barely enough energy to charge transfer, and little or no dissociation product was expected.[7,18] Only the parent ion was observed, showing that no sampling breakup was observed.

Results and Discussion

The total rate constants for reaction 1 are shown in Figure 3 as a function of pressure. No pressure dependence was found within our uncertainty of ±25%.[16] The collision rate constant is 2.0×10^{-9} cm^3 s^{-1},[25] and our measurements agree with this value within the stated uncertainty. Rate constants were not measured for all conditions since no measurable variation was found. We found that when the C_8H_{10}/N_2 reactant gas mixture was approximately older than a week, the measured rate constants would decrease, but no change was observed in the branching ratios. This result indicated that C_8H_{10} eventually absorbed on the walls of the storage vessel, thereby affecting the partial pressure. No rate constants were measured with the He buffer since the flow dynamics have not been studied in detail.

Two main product ions were observed, namely, $C_7H_7^+$ and $C_8H_{10}^+$. The former ion can exist as two isomers: tropylium, a seven-membered ring structure, and benzylium, a six-membered

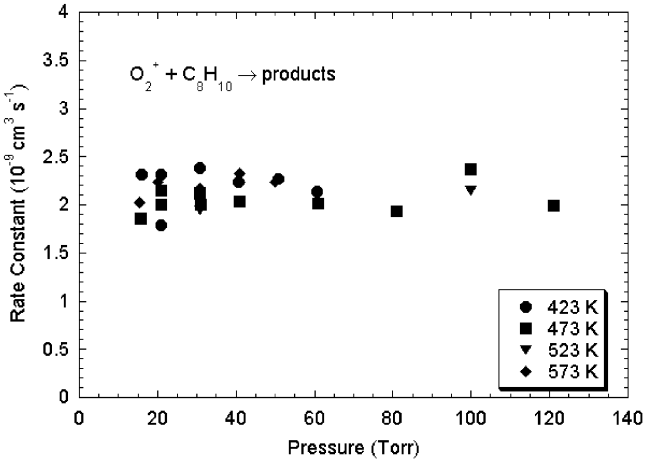

Figure 3. Rate constants as a function of pressure at various temperatures. Circles, squares, inverted triangles, and diamonds refer to 423, 473, 523, and 573 K, respectively.

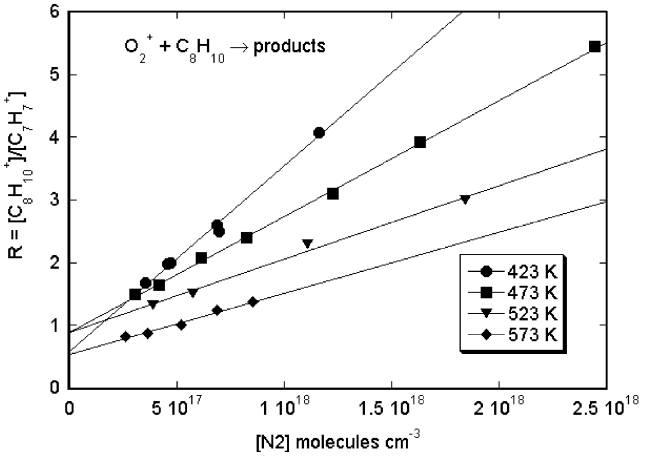

Figure 4. Ratio of [C_8H10^+] to [$C_7H_7^+$] as a function of N_2 number density at various temperatures. Circles, squares, inverted triangles, and diamonds refer to 423, 473, 523, and 573 K, respectively. Lines are linear least-squares fits through the data.

ring isomer. The present experiments do not address how much of each isomer is formed. In previous experiments, we reported that 66% of the $C_7H_7^+$ product formed from this reaction was benzylium at 300 K and 0.5 Torr.[18] Two minor products, $C_6H_6^+$ and $C_8H_9^+$, were observed; however, they were not routinely monitored nor were they reported here since their abundance was typically on the order of the impurities, i.e., <1%. The abundance of these two ions is smaller than what has been observed at low pressure, and the low abundances are consistent with the present observations of less dissociation at higher pressures. We focus on the ratio of the major product ions (R), [$C_8H_{10}^+$]/[$C_7H_7^+$], for which the small impurities have little influence. The data taken in an N_2 buffer are plotted in Figure 4 as a function of pressure at four temperatures. The pressure dependence is distinct; increasing pressure leads to more $C_8H_{10}^+$, and the effect is more pronounced at lower temperatures.

The data shown in Figure 4 are expected to be described by a linear relationship based on the following mechanism

$$\begin{aligned} O_2^+ + C_8H_{10} &\xrightarrow{\alpha k_{ct}} C_8H_{10}^+ + O_2 \\ &\xrightarrow{(1-\alpha)k_{ct}} (C_8H_{10}^+)^* + O_2 \qquad (2) \\ (C_8H_{10}^+)^* &\xrightarrow{k_q[M]} C_8H_{10}^+ + O_2 \\ (C_8H_{10}^+)^* &\xrightarrow{k_{uni}} C_7H_7^+ + CH_3 \end{aligned}$$

where k_{ct} is the total charge transfer rate constant (dissociative and nondissociative) in the absence of collisions (equal to the collision rate constant), $(C_8H_{10}^+)^*$ refers to charge transfer products with enough energy to dissociate, $(1 - \alpha)$ is the fraction of charge transfer products with enough energy to dissociate, k_{uni} is the rate constant for unimolecular dissociation (loss of CH_3) for the charge transfer product, k_q is the rate constant for collisional stabilization of the excited charge transfer product, and [M] is the total gas concentration in the tube, which is approximately equal to that of the buffer gas since [C_8H_{10}]/[M] < 10^{-5} and [O_2]/[M] ~ <10^{-2}. In this mechanism, the radiative relaxation rate is not included since it is small as compared to the unimolecular decay rate and total collisional relaxation rate under our experimental conditions. Because the reactant gas is in large excess in our experiments, i.e., [C_8H_{10}] ≫ [O_2^+], the concentration of [C_8H_{10}] is not affected by reaction.

In the limit of psuedo first-order charge transfer kinetics, the following expressions for each of the product species concentrations as a function of time can be derived

$$[(C_8H_{10}^+)^*] = [O_2^+]_o \frac{(1-\alpha)k_{ct}'}{(k_{uni} + k_q[M] - k_{ct}')}(e^{-k'_{ct}t} - e^{-(k_{uni}+k_q[M])t}) \quad (3)$$

$$[C_7H_7^+] = [O_2^+]_o \frac{(1-\alpha)k_{ct}'k_{uni}}{(k_{uni} + k_q[M] - k_{ct}')}\left[\frac{(1-e^{-k'_{ct}t})}{k_{ct}'} - \frac{(1-e^{-(k_{uni}+k_q[M])t})}{k_{uni} + k_q[M]}\right] \quad (4)$$

and

$$[C_8H_{10}^+] = [O_2^+]_o\left\{\alpha(1-e^{-k'_{ct}t}) + \frac{(1-\alpha)k_{ct}'k_q[M]}{(k_{uni} + k_q[M] - k_{ct}')}\left[\frac{(1-e^{-k'_{ct}t})}{k_{ct}'} - \frac{(1-e^{-(k_{uni}+k_q[M])t})}{k_{uni} + k_q[M]}\right]\right\} \quad (5)$$

where

$$k_{ct}' = k_{ct}[C_8H_{10}]_o \qquad (6)$$

is the pseudo first-order rate constant.

The value of k_{uni} as a function of internal energy has not been determined for $(C_8H_{10}^+)^*$, but it should be comparable to the values of $(C_7H_8^+)^*$ and $(C_9H_{12}^+)^*$, ionized toluene, and propylbenzene, respectively. For example, at a total energy of ca. 12.1 eV (see ref 7, eq 1) corresponding to reactions with O_2^+, the dissociation lifetime for $C_7H_8^+$, is approximately 20 μs whereas the dissociation lifetime ($1/k_{uni}$) for $C_9H_{12}^+$ is 0.1 μs, which is approximately 1000 times shorter than our shortest reaction time of 1.5 ms.[7,19,20] In addition, conservatively assuming that the quenching rate is small (0.01−0.001 of collision rate), k_q[M] is in the 10^6−10^7 s^{-1} range.[25] Furthermore, given an $O_2^+ + C_8H_{10}$ charge transfer rate of 2.0×10^{-9} cm^3 s^{-1} (see Figure 3) over this temperature range and a maximum C_8H_{10} concentration of ca. 10^{12} cm^{-3}, the following

TABLE 1: Slope of the Ratio, *R*, of $[C_8H_{10}^+]$ to $[C_7H_7^+]$ vs Number Density at Various Temperatures

temp (K)	buffer	slope (cm^3 $molec^{-1}$)
423	N_2	2.95×10^{-18}
473	N_2	1.85×10^{-18}
523	N_2	1.17×10^{-18}
573	N_2	9.80×10^{-19}
473	He	9.95×10^{-19}

approximations can be made under our experimental conditions

$$(k_{uni} + k_q[M])\tau \gg 1 \text{ and } (k_{uni} + k_q[M]) \gg k_{ct}' = k_{ct}[C_8H_{10}]_o \quad (7)$$

where τ is the reaction time. In essence, eq 7 indicates that the excited charge transfer product either dissociates or quenches upon formation and, hence, does not reach the detector.

Using the inequalities of eq 7 in conjunction with the concentration expressions of eqs 3−6, the ratio, $R = [C_8H_{10}^+]/[C_7H_7^+]$, simplifies to the following expression

$$R = [C_8H_{10}^+]/[C_7H_7^+] = \frac{\alpha}{1-\alpha} + \frac{k_q[M]}{(1-\alpha)k_{uni}} \quad (8)$$

Equation 8 shows that under our experimental conditions, *R* should depend linearly on the buffer gas density. Least-squares lines shown in Figure 4 show that linear dependences with [M] are indeed good representations of the pressure or number density dependence. According to eq 8, the slopes are the ratio of the bimolecular quenching rate constant to the unimolecular dissociation rate, divided by the fraction of the overall reaction that produces an excited species. The slopes, which are listed in Table 1, decrease with increasing temperature. These values are plotted in Figure 5 as a function of temperature. The data are fit to a power law and the least-squares line is drawn through the data. The data are well-represented by this fit. The temperature dependence of the slope is $T^{-3.75}$ with a correlation coefficient of 0.995.

The zero pressure intercepts should yield the low-pressure value of the branching ratio. To test this, we have measured the ratio in 0.2 Torr N_2 at 473 K in the selected ion flow tube in our laboratory and found a ratio of 0.33, in excellent agreement with the value obtained previously in He.[7,18] In a single collision high-temperature guided ion beam apparatus, values of 0.28 and 0.20 were found at temperatures of 300 and 600 K, respectively.[7] The intercepts in the pressure studies are close to but higher than these values, and no trend is discernible. As outlined in the Experimental Section, tests were performed on essentially every experimental condition that could be varied with no effect on the results. Therefore, we do not try to interpret the intercepts.

Data were also taken in He at three temperatures. Figure 6 shows data in both He and N_2 buffers with only a subset of the N_2 data plotted for clarity. In He, only one pressure dependence was performed due to the amount of He that was required, i.e., three full-sized cylinders of He were expended to obtain the data shown here. At all temperatures, *R* is larger in N_2 than in He although the difference is very small at 573 K, primarily because neither buffer gas is very efficient at quenching the dissociation at high temperatures. Comparing the number density dependences at 473 K, we find the slope in N_2 to be 1.86 times that of He. The unimolecular dissociation rate must be the same since the ions are formed in the same manner. Thus, the quenching rate for N_2 is almost twice as large as for He. Part of this dependence is due to the collision rate difference for the

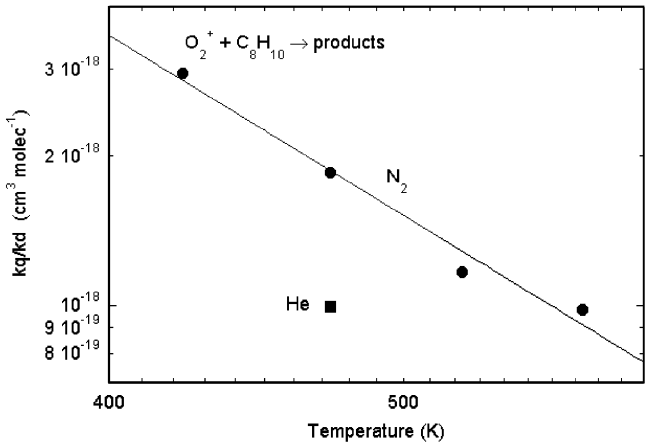

Figure 5. $(1/1 - \alpha)k_q/k_{uni}$ values deduced from the data slopes shown in Figures 4 and 6 vs gas temperature. Circles and squares refer to data taken in N_2 and He buffers, respectively. The line is a power law fit to the N_2 buffer data.

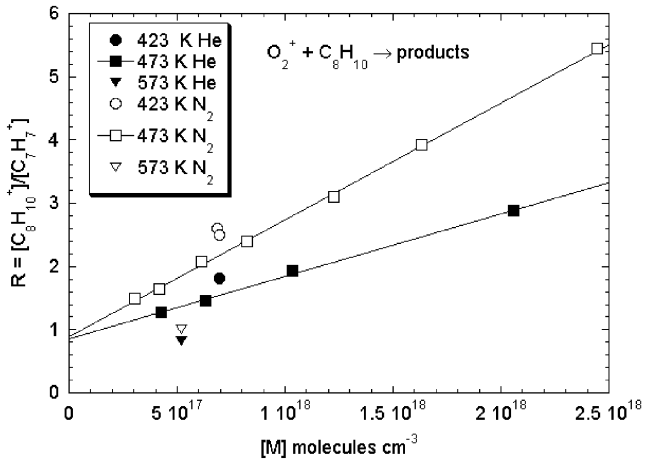

Figure 6. Ratio of $[C_8H10^+]$ to $[C_7H_7^+]$ as a function of number density at various temperatures. Circles, squares, and inverted triangles refer to 423, 473, and 573 K, respectively. Open and solid points refer to data taken in N_2 and He buffers, respectively. Lines are linear least-squares fits to the data. Only a portion of the N_2 data is shown for clarity.

two partners. According to the Langevin theory,[26] N_2 should collide with the ion complex 1.18 times more often than He at the same number density. Accounting for this effect, N_2 is still 1.56 times more efficient than He at quenching the dissociation per collision. Nitrogen is known to be more effective at quenching than is He.[27−30] For instance, Ahmed and Dunbar find that N_2 is 2.14 times as efficient as He in quenching excited bromobenzene cations after accounting for the difference in collision rates.[29] Miasek and Harrison found that N_2 is 1.69 times more efficient than He in quenching $(C_5H_9^+)^*$.[30]

Previously in a high-temperature flowing afterglow study of the reaction of NO^+ with C_8H_{10},[7] it was shown that $C_8H_{10}^+$ thermally dissociated at temperatures above approximately 650 K in 1 Torr of He. At higher pressures, the onset of dissociation should occur at lower temperatures, since the rate depends on pressure (linearly in the low-pressure limit). For the present experiments, 573 K was the maximum possible temperature that could be achieved. To test for the possibility of thermal dissociation of $C_8H_{10}^+$ at 573 K, the branching ratio was measured at two reaction distances at 40 Torr N_2 gas pressure. Shorter distance leaves less dissociation time and therefore should favor $C_8H_{10}^+$ over $C_7H_7^+$. There was a very slight difference between data taken with the injector at 35 cm (55%

$C_8H_{10}^+$) and 70 cm (52% $C_8H_{10}^+$). This translates into *R* values of 1.22 and 1.08, respectively, the latter being shown in the graphs and tables. Thus, it appears that a small amount of thermal dissociation is occurring. However, the difference is small and barely detectable.

At slightly higher temperatures, thermal dissociation of $C_8H_{10}^+$ will probably be more important than the collisional stabilization observed in the present study. Therefore, as the temperature is raised, a competition between quenching and thermal activation will occur. Eventually, the slopes of *R* should become negative. From the low-pressure experiments of NO^+ with C_8H_{10} and the test described above at 573 K, one would expect the slopes to become negative at temperatures only slightly higher than 573 K.

Conclusions

The first measurements taken in the upgraded TIFT as a function of both temperature and pressure are reported. Few other instruments are capable of such measurements,[31] and this is the only instrument to combine such capabilities with the advantages inherent to flow tubes. For instance, the experiments reported here would probably be limited by impurities in (quasi) static systems. Flexibility in ion production is greater, and studies involving reactive neutrals are possible.[16] Low-pressure measurements in conventional flow tubes and other still lower pressure ion instruments generally measure true bimolecular rate constants, although recent work has shown that exceptions may occur regularly at pressures on the order of 1 Torr. Because many plasmas occur at elevated pressure, it is important to extend the pressure range upward.

The measurements reported here for the reaction of O_2^+ with ethylbenzene confirm previous conclusions regarding the importance of buffer effects in the competition between charge transfer and dissociative charge transfer for the reactions of alkylbenzenes and simple ions.[7,18] Increasing pressure dramatically changes the amount of dissociation. The pressure dependence of the ratio of nondissociative charge transfer products to dissociative charge transfer, *R*, increases linearly over the experimental range reported here. A simple model predicts such a dependence. Increasing temperature decreases the importance of the buffer, although the onset of a thermal dissociation process is probably observed at the highest temperature. This leads to a situation where the pressure dependence of *R* is steep and positive at low temperature. The slope gradually decreases with increasing temperature and is expected to become negative at temperatures higher than the current upper limit. Thus, to fully understand such reactions, studies must be conducted over as wide a range of conditions as possible.

The present results will have an impact on the inputs to models of plasma-enhanced combustion.[32,33] However, combustion takes place at even higher temperatures and pressures than the current experimental limitations allowed. Neither the ability to heat the buffer to higher temperatures nor the elimination of impurities is an inherent obstacle to higher temperature and/or pressure operation. Therefore, further upgrades to the TIFT should allow for operation up to approximately 900 K and pressures up to approximately one atmosphere. This will be the second highest temperature of current generation ion−molecule apparatus.[34,35] Combining that capability with the extended pressure variability will be unique and should allow for many interesting studies.

Acknowledgment. We thank John Williamson and Paul Mundis for technical support. T.M.M. is supported through Visidyne contract number F19628-99-C-0069. This work is supported by AFOSR under Task 2303EP4.

References and Notes

(1) Arnold, S. T.; Williams, S.; Dotan, I.; Midey, A. J.; Morris, R. A.; Viggiano, A. A. *J. Phys. Chem. A* **1999**, *103*, 8421.
(2) Midey, A. J.; Williams, S.; Arnold, S. T.; Dotan, I.; Morris, R. A.; Viggiano, A. A. *Int. J. Mass Spectrom.* **2000**, *195*, 327.
(3) Jochims, H. W.; Rasekh, H.; Ruhl, E.; Baumgartel, H.; Leach, S. *Chem. Phys.* **1992**, *168*, 159.
(4) Sell, J. A.; Mintz, D. M.; Kuppermann, A. *Chem. Phys. Lett.* **1978**, *58*, 601.
(5) Kuhlewind, H.; Kiermeier, A.; Neusser, H. J. *J. Chem. Phys.* **1986**, *85*, 4427.
(6) Ho, Y. P.; Dunbar, R. C.; Lifshitz, C. *J. Am. Chem. Soc.* **1995**, *117*, 6504.
(7) Williams, S.; Midey, A. J.; Arnold, S. T.; Morris, R. A.; Viggiano, A. A.; Chiu, Y.-H.; Levandier, D. J.; Dressler, R. A.; Berman, M. R. *J. Phys. Chem. A* **2000**, *104*, 10336.
(8) Midey, A. J.; Williams, S.; Arnold, S. T.; Viggiano, A. A. *J. Phys. Chem. A*, submitted for publication.
(9) Seeley, J. V.; Morris, R. A.; Viggiano, A. A.; Wang, H.; Hase, W. L. *J. Am. Chem. Soc.* **1997**, *119*, 577−584.
(10) Arnold, S. T.; Morris, R. A.; Viggiano, A. A. *J. Chem. Phys.* **1995**, *103*, 9242.
(11) Hierl, P. M.; Ahrens, A. F.; Henchman, M.; Viggiano, A. A.; Paulson, J. F. *Int. J. Mass Spectrom. Ion Phys.* **1987**, *81*, 101.
(12) Viggiano, A. A.; Arnold, S. T.; Morris, R. A. *Int. Rev. Phys. Chem.* **1998**, *17*, 147−184.
(13) Sieck, L. W.; Meot-Ner (Mautner), M. *J. Phys. Chem.* **1984**, *88*, 5324.
(14) Sieck, L. W.; Meot-Ner (Mautner), M. *J. Phys. Chem.* **1984**, *88*, 5328.
(15) Meot-Ner (Mautner), M.; Hunter, E. P.; Field, F. H. *J. Am. Chem. Soc.* **1977**, *99*, 5576.
(16) Arnold, S. T.; Seeley, J. V.; Williamson, J. S.; Mundis, P. L.; Viggiano, A. A. *J. Phys. Chem. A* **2000**, *104*, 5511.
(17) Arnold, S. T.; Viggiano, A. A. *J. Phys. Chem. A* **2001**, *105*, 3527.
(18) Arnold, S. T.; Dotan, I.; Williams, S.; Viggiano, A. A.; Morris, R. A. *J. Phys. Chem. A* **2000**, *104*, 928−934.
(19) Huang, F.-S.; Dunbar, R. S. *Int. J. Mass Spectrom. Ion Processes* **1991**, *109*, 151−170.
(20) Hwang, W. G.; Moon, J. H.; Choe, J. C.; Kim, M. S. *J. Phys. Chem. A* **1998**, *102*, 7512−7518.
(21) Gilbert, M. *Combust. Flame* **1958**, *2*, 149.
(22) Miller, T. M.; Ballenthin, J. O.; Meads, R. F.; Hunton, D. E.; Thorn, W. F.; Viggiano, A. A.; Kondo, Y.; Koike, M.; Zhao, Y. *J. Geophys. Res.* **2000**, *105*, 3701−3707.
(23) Hunton, D. E.; Ballenthin, J. O.; Borghetti, J. F.; Federico, G. S.; Miller, T. M.; Thorn, W. F.; Viggiano, A. A.; Anderson, B. E.; Cofer, W. R.; McDougal, D. S.; Wey, C. C. *J. Geophys. Res.* **2000**, *105*, 26, 841−26, 855.
(24) Ausloos, P.; Jackson, J.-A. A.; Lias, S. G. *Int. J. Mass Spectrom. Ion Phys.* **1980**, *33*, 269−283.
(25) Su, T.; Chesnavich, W. J. *J. Chem. Phys.* **1982**, *76*, 5183−5185.
(26) Gioumousis, G.; Stevenson, D. P. *J. Chem. Phys.* **1958**, *29*, 294−299.
(27) Viggiano, A. A. *J. Chem. Phys.* **1984**, *81*, 2639.
(28) Viggiano, A. A.; Dale, F.; Paulson, J. F. *J. Geophys. Res.* **1985**, *90*, 7977.
(29) Ahmed, M. S.; Dunbar, R. C. *J. Am. Chem. Soc.* **1987**, *109*, 3215−3219.
(30) Miasek, P. G.; Harrison, A. G. *J. Am. Chem. Soc.* **1975**, *97*, 714.
(31) Knighton, W. B.; Grimsurd, E. P. Gas-Phase Ion Chemistry Under Conditions of Very High Pressure. In *Advances in Gas-Phase Ion Chemistry*; Adams, N. G., Babcock, L. M., Eds.; JAI Press: Greenwich, CT, 1996; Vol. 2, pp 219−258.
(32) Williams, S.; Midey, A. J.; Arnold, S. T.; Miller, T. M.; Bench, P. M.; Dressler, R. A.; Chiu, Y.-H.; Levandier, D. J.; Viggiano, A. A.; Morris, R. A.; Berman, M. R.; Maurice, L. Q.; Carter, C. D. Progress on the investigation of the effects of ionization on hydrocarbon/air combustion chemistry: kinetics and thermodynamics of C6−C10 hydrocarbon ions; AIAA 4th Weakly Ionized Gases Workshop, Anaheim, California, 2001.
(33) Williams, S.; Bench, P. M.; Midey, A. J.; Arnold, S. T.; Viggiano, A. A.; Morris, R. A.; Maurice, L. Q.; Carter, C. D. Detailed Ion Kinetic Mechanisms for Hydrocarbon/Air Combustion Chemistry. In *JANNAF Publication No. 703 entitled 37th Combustion, 25th Airbreathing Propulsion, 1st Modeling and Simulation Subcommittees*, Monterey, CA, 2000; Vol. 1, pp 205−213.
(34) Viggiano, A. A. Instrumentation−Ion Chemistry at High Temperature. In *Encyclopedia of Mass Spectrometry−Ion Chemistry*; Armentrout, P. B., Ed.; Elsevier Science: New York, 2003; Vol. 5.
(35) Hierl, P. M.; Friedman, J. F.; Miller, T. M.; Dotan, I.; Mendendez-Barreto, M.; Seeley, J.; Williamson, J. S.; Dale, F.; Mundis, P. L.; Morris, R. A.; Paulson, J. F.; Viggiano, A. A. *Rev. Sci. Instrum.* **1996**, *67*, 2142.